P. TREBUŇA, M. PÁSTOR, F. TREBUŇA, F. ŠIMČÁK

ISSN 0543-5846
METABK 56(1-2) 233-236 (2017)
UDC – UDK 621-25:621.165.DO464:66.014:620.17=111

THE ANALYSIS OF FAILURE CAUSES OF THE ROTOR SHAFT OF STEAM TURBINES

Received – Primljeno: 2016-05-25
Accepted – Prihvaćeno: 2016-10-10
Preliminary Note – Prethodno priopćenje

The rotors of steam turbines belong to the extremely loaded parts of turbo generators due to various mechanical and thermal influences during their operation. The following paper presents the results of the analysis of failure causes of the rotor shaft of a steam turbine with the power of 6,43 MW, which occurred after approximately one year of operation. The analysis was performed on the basis of the analysis of the chemical composition and microstructure of the material, the mechanical properties of the material under static and fatigue loading, as well as operational loading of the critical location of the shaft, using numerical and analytical methods. The conclusions about the possible causes of the shaft failure were drawn on the basis of the results obtained.

Key words: rotor, steam turbine, failure, chemical composition, mechanical properties

INTRODUCTION

Electricity is often produced by steam turbo generators consisting of a steam turbine, reduction gear and a generator [1, 2]. The source of energy is steam, expanding in multiple stages in a steam turbine, where rotating blades cause the rotation of the turbine rotor. The rotation frequencies of steam turbines with turbo generators are, in general, derived from the parameters of the generator (the most frequently 25 or 50 Hz). In case of a small steam turbine with a power output of approximately 30 MW, reduction gears are used to increase the rotation frequency of the turbine rotor, up to about 10^4 rpm.

Due to the fact that the steam can reach the pressure of several tenths of MPa, with the temperature near 400 °C on the input of the turbine, turbine rotors (shafts with rotating blades) belong to extremely loaded parts of turbines because of severe mechanical and thermal influences. Even though the turbine rotors are made of special alloy steels, produced with modern production technologies under quality control systems, shafts and blades are frequently the source of failure of this equipment [3 - 6]. The cause of failures is analysed by analytical, numerical, as well as experimental methods of mechanics and material science [7, 8].

The paper presents a procedure for the analysis aiming to identify the causes of the failure of the steam turbine rotor shaft. The turbine is part of the steam turbo generator used for the production of electrical energy. The steam turbo generator with the reduction gear has the power of 6,43 MW with 8 200 rpm.

The analysed turbo generator consists of a steam turbine, reduction gear and a generator for the production of electrical energy. The shaft of the turbine rotor (Figure 1) is positioned in two radial bearings. Axial movement of the shaft is limited by axial bearing. The shaft is forged as a whole with T-grooved discs, for the positioning of blades.

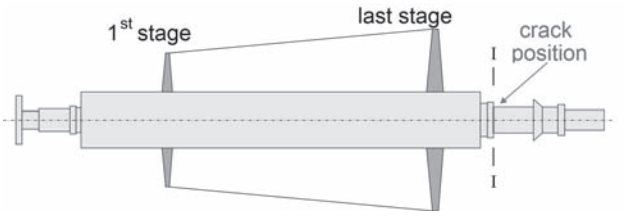

Figure 1 Shaft of turbine rotor

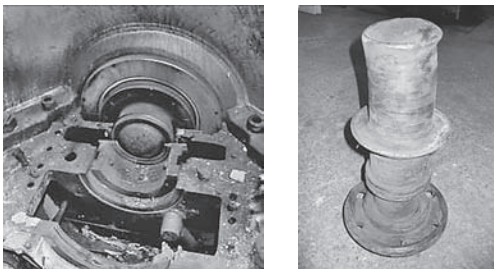

Figure 2 a) View of the fracture surface on the side of turbine, b) view of the broken part of turbine shaft

After a relatively short operation time (approximately one year), a failure of the turbine rotor shaft occurred, when it broke in the cross-section I - I (Figure 1). Figure 2a shows a view of the fracture surface of the shaft from the side of the turbine. Figure 2b gives a view of the broken part of the turbine shaft.

THE ANALYSIS OF THE FRACTURED SURFACE OF THE SHAFT FROM THE POINT OF VIEW OF FAILURE MECHANISMS

Figure 3 gives details of the fracture surface of the shaft from the side of the turbine and Figure 4 shows the

P. Trebuňa, M. Pástor, F. Trebuňa, F. Šimčák, Technical university of Košice, Faculty of Mechanical Engineering, Košice, Slovakia

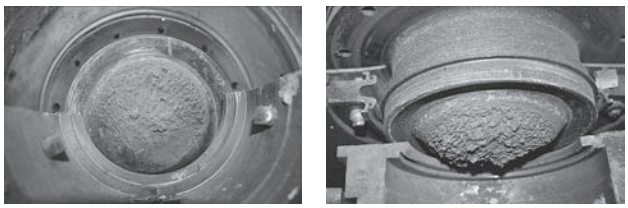

a) b)

Figure 3 Details of the fracture surface of the shaft from the side of turbine

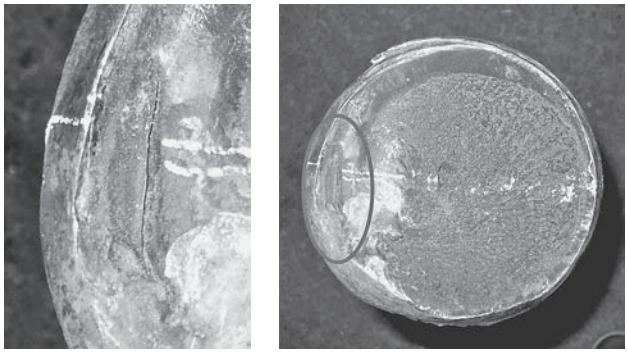

a) b)

Figure 4 Fracture surface on broken part of shaft

fracture surface on the broken part of the shaft. As Figures 3,4 show, the fracture surface exhibits the area of fatigue damage (glossy part of the cross-section on the periphery of the surface) in the shape of an eccentric circular ring and the internal area of brittle fracture.

In the location, where the area of fatigue damage is broader (left side of the fracture surface in Figure 4b), an approximately 30 mm long macro fracture is visible in the circumferential direction at the distance of approximately 15 mm under the surface of the shaft (Figure 4a). A more detailed insight into the macro fracture (Figure 5) leads to the conclusion that it is a strip introduced during forging of the shaft.

The initiation of fatigue damage in the circumferential direction of the shaft cross-section proves that its spreading in the cross-section is caused by combined loading of the bending moment and torque. The crack in the cross-section was initiated by the above mentioned stress concentrator strip that together with the sharp groove on the surface of the shaft, localizes the area of the first failure of the turbine rotor shaft. The location of fatigue crack initiation is seen in Figure 5.

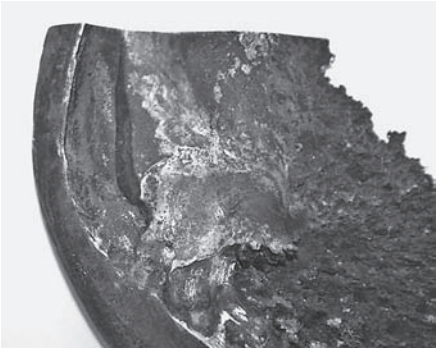

Figure 5 Detail of macro fracture

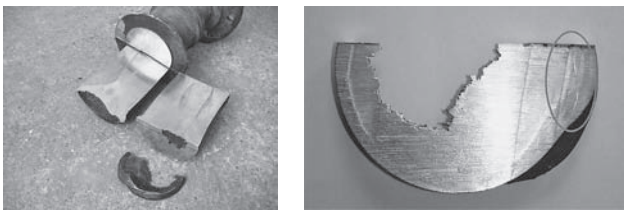

a) b)

Figure 6 a) material taken from the broken part of turbine shaft, b) view of the separated end segment from the side of cross-section with crack

SELECTED MECHANICAL PROPERTIES OF TURBINE SHAFT MATERIAL

The following analyses and tests were performed in order to identify selected material parameters of the turbine shaft:

- Analysis of chemical composition, metallographic analysis;
- Static tensile tests;
- Hardness and notch toughness tests;
- Fatigue tests under cyclic symmetric loading by torque and plane bending.

The material for tests was taken from the broken part of the shaft Figure 6a, while from the sample of the material, the end segment, on which the fatigue part of the fracture with a macro crack (strip) lay, was separated. The separated end segment (Figure 6b) provided evidence that the strip as a result of inappropriate technology of forging created a groove that in some locations ran to the surface of the shaft.

The chemical composition of the shaft material determined by spectrometer is given in Table 1.

Table 1 **The chemical composition of the shaft material / wt %**

Fe	C	Si	Mn	Cr	Mo	Ni
94,61	0,278	0,011	0,325	1,48	0,353	2,734
Cu	P	S	Al	V	Ti	Nb
0,059	0,002	0,002	0,006	0,117	0,002	0,013

The measured chemical composition corresponds in the tables of materials to steel with the prescribed chemical composition given in Table 2 by STN 41 6431 [9] (equivalents according to foreign standards are 26NiCrMo8-5, or SEW555-84).

Table 2 **Prescribed chemical composition of steel STN 41 6431 / wt %**

C	Mn	Si	Cr	Ni
0,25 - 0,32	0,4 - 0,6	max. 0,37	1,2 - 1,6	1,8 - 2,3
Mo	V	Cu	P	S
0,35 -0,45	0,05 -0,10	max. 0,2	max. 0,035	max. 0,035

The microstructure of the shaft is given in Figure 7. It consists of tempered martensite – sorbit, which provides evidence of a suitable technology of thermal processing.

The basic mechanical properties of the shaft material were determined by the static tensile test. The inter-

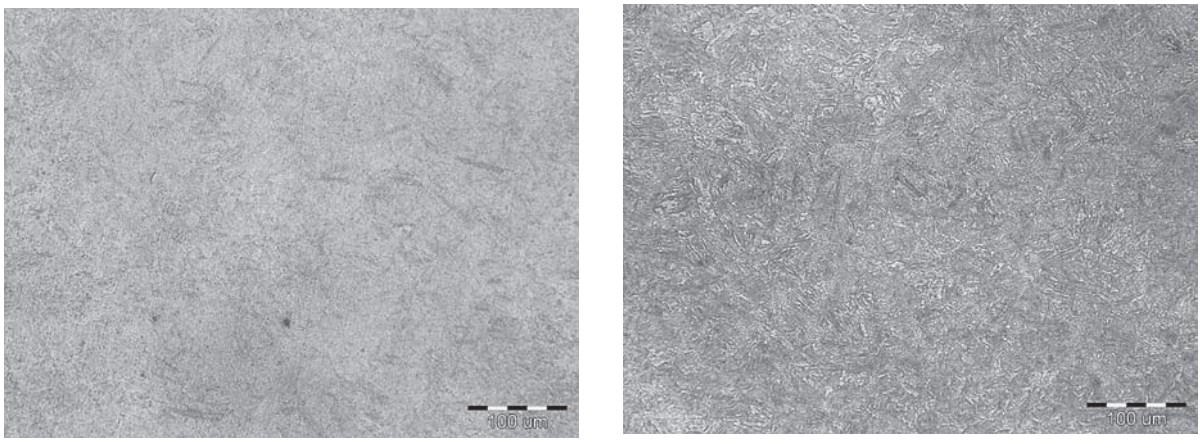

a) b)

Figure 7 View of the microstructure. a) in direction of shaft axis, b) perpendicular to shaft axis

vals of values from three measurements on the samples oriented in the direction of the shaft are given in Table 3. The table also gives the prescribed values of mechanical properties for material 16 431.

Table 3 **The mechanical properties of shaft material**

	$R_{p0,2}$ / MPa	R_m / MPa	A_5 / %	Z / %
Measure values	613 – 662	769 – 789	20,7 – 22,3	71,4 – 73,4
Material 16 431	min 569	686-834	min 20	-

The hardness according to Brinell, reaches the magnitudes of 247÷257 HBS where the prescribed values for material 16431 are 208÷253 HBS. The notch toughness of the material was determined by a pendulum hammer. The measurements on the three samples with V-grooves gave us values in the range KCV = 209÷233 Jcm^{-2} and the measurements on the three samples with U-grooves was in the interval KCU = 243÷251 Jcm^{-2}. The minimal prescribed value for material 16431 is KCU = 78 Jcm^{-2}.

The fatigue material properties of the turbine shaft were evaluated for cyclic symmetric loading by torsion, as well as for cyclic symmetric plane bending [8]. The fatigue limit for torsion was $\tau_c = \pm 181$ MPa and the fatigue limit and strength ratio was $\tau_c/R_m = 0{,}233$. Fatigue limit and yield stress ratio was $\tau_c/R_e = 0{,}283$.

The fatigue limit for plane bending was $\sigma_{co} = \pm 330$ MPa. Fatigue limit for plane bending and strength ratio was $\sigma_{co}/R_m = 0{,}423$. Fatigue limit for plane bending and yield stress ratio was $\sigma_{co}/R_e = 0{,}516$.

The measured fatigue characteristics σ_{co}, τ_c, their ratio to the tensile strength and to yield stress, correspond to the state of the shaft material and they are in accordance with the properties of similar steels, e.g., 16 310.6, or 16 343.6.

CONCLUSION

On the basis of the performed analyses, it can be stated that:

- The analysis of the fracture surface of the shaft showed that the location with the deepest fatigue crack contained a crack in the circumferential direction, the initiation of which could not be connected with loading, but with inappropriate production technology of the turbine rotor. With high probability, these problems were connected with the presence of a strip that resulted from forging. This crack led to a sharp notch on the surface and under variable loading, it caused the failure of the shaft.
- The chemical composition of the shaft material corresponded to the material STN 41 6431 (equivalent to 26NiCrMo8-5-SEW 555-84), where the microstructure of the material indicates the suitability of the technology used for thermal processing of the machine part. It is necessary to mention that according to the material description [9], this steel is suitable for rotors of electrical generators and it does not have prescribed mechanical properties for the temperatures under which the analysed steam turbine works.
- The mechanical properties were determined for tensile loading. The measurements were performed for three specimens, and magnitudes of yield stress $R_{p0,2}$, strength R_m as well as plastic properties A_5 and Z, were measured. Average values from three specimens were $R_{p0,2}$ = 640 MPa and R_m = 778 MPa. These values represented a basis for the assessment of the shaft strength capacity under loading and failure conditions. The fatigue properties were investigated for cyclic symmetric loading by bending and torque. The number of cycles, up to the failure, was measured from ten samples for the first, as well as second, loading type. Consequently, the Wöhler curves were designated with the fatigue limit for bending σ_{co} = 330 MPa and the fatigue limit for torsion τ_c = 181 MPa.
- From the comparison of the mechanical properties of the shaft and maximum stress values computed in the location of the notch, it follows that the weakening of the cross-section by the strip did not lead to the shaft failure. The failure was caused by additional bending loading that could result from various sources. One of the reasons could be connected with the non-parallel

positions of the gear input shaft and the turbine rotor shaft. However, the eccentricity could not be confirmed through inspection, because the bearings were completely damaged. Another reason could be connected with exceeded vibrations caused by the eccentricity or unbalance of the rotor (e.g. caused by material stuck to the turbine blades), released anchoring, due to damage of the bearing or by axial movement of the rotor. Extreme vibration could also be caused by inappropriate fixation of the input pipes to the supporting structure. Failure of blades or discs that carried the blades, could also lead to excessive turbine vibration.

Acknowledgement

This paper was supported by the projects of the Slovak Grant Agency, VEGA No. 1/0751/16 and No. 1/0393/14.

REFERENCES

[1] P. Heinz, B. Murari, P. Singh, Steam Turbines: Design, Applications, and Rerating, Second Edition. New York, 2009 The McGraw-Hill Companies, Inc., ISBN 9780071508216

[2] A. Leyzerovich, *Steam turbines for modern fossil-fuel power plants*, 2008. Lilburn: The Fairmont Press, Inc., ISBN 0-88173-548-5.

[3] S. Barella, M. Bellogini, M. Boniardi, S. Cincera, Failure analysis of a steam turbine rotor. Engineering Failure Analysis 18 (2011) 6, 511-519

[4] I. Sărăcin, G. Paraschiv, O. Pandia, I. Bozgă, D. Toma, Researches on corrosion cracking phenomenon that occurs on welded of agricultural equipment. Metalurgija 54 (2015) 2, 395 – 398

[5] Z. Mazur, R. G. Illescas, J. A. Romano, N. P. Rodrigue, Steam turbine blade failure analysis. Engineering Failure Analysis 15 (2008) 1 - 2, 129-141

[6] E. Poursaeidi, M. R. Mohammadi Arhani, Failure investigation of an auxiliary steam turbine. Engineering Failure Analysis 17 (2010) 6, 1328 - 1336

[7] F. Trebuňa, F. Šimčák, J. Bocko, P. Trebuňa, Identification of causes of radial fan failure. Engineering Failure Analysis 16 (2009) 7, 2054 - 2065

[8] F. Trebuňa, F. Šimčák, Odolnosť prvkov mechanických sústav. EMILENA, Košice, 2004.

[9] I. Fűrbacher, K. Macek, J. Steidl, Lexikon technických materiálů. Svazek 1, Verlab Dashőfer, 2005.

Note: English language: Mgr. Marcela Chabová, PhD., Košice, Slovakia